Identification of Numerical Iron-Loss Model Parameters from Electrical Steel Manufacturer Specifications

P. Rasilo*, A. Abdallh†, A. Belahcen*, and L. Dupré†

*Dept. of Electrical Engineering and Automation, Aalto University, P.O. Box. 13000, 00076, Espoo, Finland
†Dept. of Electrical Energy, Systems & Automation, Ghent University, Sint-Pietersnieuwstr. 41, 9000 Gent, Belgium
E-mail: paavo.rasilo@aalto.fi

***Abstract*—This paper deals with parameter identification for a numerical iron-loss model for electrical steel sheets. The model comprises a solution for the eddy currents in the sheet thickness, a Jiles-Atherton hysteresis model and a dynamic model for the excess eddy currents. We study if an accurate loss model can be obtained by estimating the parameter values using only the 50-Hz single-valued magnetization and loss-density curves typically provided by electrical steel manufacturers. The optimal parameter values are searched as a solution of an experimental-numerical inverse problem. The accuracy of the loss prediction at higher frequencies is then quantified. It is found that if the conductivity of the material is not known, the solution of the inverse problem is not unique. However, if the conductivity is known, the other loss-model parameters can be recovered with good accuracy.**

***Index Terms*—Electromagnetic inverse problems, iron losses, magnetic materials.**

I. Introduction

Prediction of power losses in laminated magnetic cores of electromagnetic devices has remained challenging up to this date. The losses have traditionally been estimated by Steinmetz's experimental formula [1] or the statistical loss-segregation theory of Bertotti [2]. Bertotti's theory segregates the losses into static hysteresis, macroscopic or *classical* eddy-current and *excess* eddy-current losses. For a sinusoidal flux density with an amplitude $\hat{b}$ and frequency $\omega = 2\pi f$, the average iron-loss power density over a full cycle is rather accurately given by the sum of the three components, respectively:

$$p = f w_{\text{hy}}(\hat{b}) + \frac{\sigma d^2}{24}(\omega\hat{b})^2 + c_{\text{ex}}(\omega\hat{b})^{\frac{3}{2}}. \qquad (1)$$

Here w_{hy} is the rate-independent hysteretic energy loss, σ is the electrical conductivity, d the lamination thickness, and c_{ex} is a coefficient describing the loss related to the excess eddy currents. The classical eddy-current loss given by the middle term is calculated analytically with the assumption that the skin-effect in the lamination thickness can be neglected [3].

In the case of non-sinusoidal supply, (1) as such cannot be used. Instead, several more or less experimental approaches have been presented for obtaining the instantaneous losses during arbitrary time variation [4]–[6]. However, coupling the iron losses to numerical analysis tools for electromagnetic devices requires modeling not the instantaneous loss but the relationship between average flux density $b_0(t)$ and the surface field strength $h_{\text{s}}(t)$ in the sheet. If the skin effect is neglected, the approach proposed in [7] can be used. The surface field is divided into hysteretic, classical and excess parts as

$$h_{\text{s}} = h_{\text{hy}}\left(b_0\right) + \frac{\sigma d^2}{12}\frac{\partial b_0}{\partial t} + c_{\text{ex}}\left|\frac{\partial b_0}{\partial t}\right|^{-0.5}\frac{\partial b_0}{\partial t}, \qquad (2)$$

which gives the average loss densities equally to (1) in the case of sinusoidal $b_0(t)$. With higher frequencies, however, the skin effect cannot be neglected, and the most accurate results are obtained by numerically modeling the actual physical behavior of the flux density in the lamination [8]–[11]. Such models are derived starting from the quasistatic Maxwell equations, which, assuming an infinitely large core lamination, reduce to a 1-D diffusion equation for the flux density $b(z,t)$ and field strength $h(z,t)$ in the lamination thickness $z \in [-d/2, d/2]$:

$$\frac{\partial^2 h(z,t)}{\partial z^2} = \sigma\frac{\partial b(z,t)}{\partial t}. \qquad (3)$$

To account for all the three loss components in (1), the local $h\left(b\left(z,t\right)\right)$ relationship should include models for both static hysteresis and the local excess eddy currents. The static hysteresis part is most often modeled either by a Preisach model [8], [9], [11] or a Jiles-Atherton (J-A) model [10]. The Everett map required for the Preisach model can be built from measured first-order reversal curves (FORCs), which requires a lot of experimental work. On the other hand, the Jiles-Atherton model makes certain assumptions on the anhysteretic curve shape, but still requires identification of five constants based on static hystesis loop measurements. In addition, although the conductivity of the lamination material may often be known, identification of the excess loss coefficient c_{ex} requires measurements at different frequencies. However, the data provided by the electrical steel manufacturer is typically limited to the single-valued magnetization properties $\hat{h}(\hat{b})$ and loss densities $p(\hat{b})$ measured at 50-Hz sinusoidal flux-density excitation (Fig. 1). Therefore, the complete identification procedure for the parameters of an iron-loss model is a rather complex process and requires a big effort from the user [8], [12]. This is one

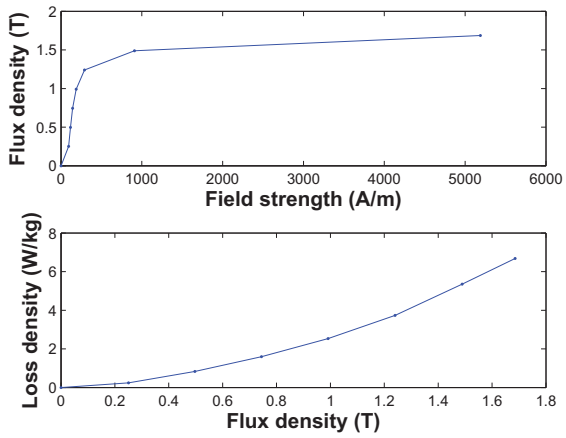

Fig. 1. Typical single-valued magnetization and loss-density data provided by electrical steel manufacturers (measured from the ring-core setup described in Section II A).

of the reasons why accurate physical modeling of power losses has not become everyday routine for design and research of electromagnetic devices.

Ideally, the loss models should be identifiable merely from the manufacturer data without additional measurements. In [13], this was attempted for the static hysteretic part using a Preisach model and an analytical expression for the FORCs. The excess losses were neglected and the classical eddy-current losses were subtracted from the 50-Hz loss-density data. Although the results were in good agreement with the loss data from the manufacturer, the predicted losses at higher frequencies were not compared to measurements. In [4], loss tables for sinusoidal excitation provided by the manufacturer were used to predict losses in high-frequency power-electronic transformers with arbitrary current waveforms. However, the applied loss models were rather experimental in nature.

In this paper, we formulate the parameter identification from the data of Fig. 1 as a coupled experimental-numerical inverse problem [14], [15]. The 50-Hz magnetization and loss-density curves are physically modeled by numerically solving (3). Hysteresis is modeled with a J-A model in which the number of parameters is reduced to three by interpolating the anhysteretic magnetization curve from the 50-Hz measurements. The remaining five parameters of the iron-loss model are solved by iteratively minimizing the difference between the simulations and experiments with a standard ring-core setup. It is found that the solution is non-unique if the conductivity of the material is not known. However, with a known conductivity, the parameters identified from the 50-Hz data also give good prediction accuracy for the loss densities at higher frequencies.

II. Methods

A. Ring-Core Measurements

A standard ring-core setup was used to measure the 50-Hz manufacturer-like curves for identification purposes and high-frequency loss densities for validation purposes. The core is stacked of 20 0.5-mm thick rings cut with electrical discharge machining from non-oriented M530/50A electrical steel. The conductivity of the material is $\sigma = 2.96$ MS/m. The inner and outer radii of the rings are 45 and 55 mm, respectively. The core is equipped with both primary and secondary windings for magnetic-field and flux-density measurements according to IEEE Standard 393-1991. The measurements were performed under controlled sinusoidal flux-density excitation at several amplitudes and frequencies of 50, 100 200 and 300 Hz.

B. Numerical Iron-Loss Model

In the numerical solution of (3), the flux-density distribution in the lamination thickness is approximated by a truncated cosine series:

$$b(z,t) = \sum_{n=0}^{N_\mathrm{b}-1} b_n(t)\alpha_n(z) \tag{4}$$

with $\alpha_n(z) = \cos\left(2n\pi\frac{z}{d}\right)$. To fulfill (3) identically, the field strength is expanded as

$$\tilde{h}(z,t) = h_\mathrm{s}(t) - \sigma d^2 \sum_{n=0}^{N_\mathrm{b}-1} \frac{\partial b_n(t)}{\partial t}\beta_n(z), \tag{5}$$

where $h_\mathrm{s}(t)$ is the field strength on the lamination surface and the functions $\beta_n(z)$ are defined so that $\beta_n(\pm d/2) = 0$ and

$$\alpha_n(z) = -d^2\frac{\partial^2\beta_n(z)}{\partial z^2}. \tag{6}$$

With a finite number of terms in the series expansion, $\tilde{h}$ does not satisfy the constitutive material law $h(b)$ which is therefore expressed weakly with respect to the basis functions as

$$\frac{1}{d}\int_{-d/2}^{d/2}\left[\tilde{h}(z,t) - h(b(z,t))\right]\alpha_n(z)dz = 0 \tag{7}$$

for $n = 0,\ldots,N_\mathrm{b}-1$. Substituting (5) and solving the surface field strength yields the following system of equations describing the behavior of the field in the lamination:

$$\begin{bmatrix} h_\mathrm{s}(t) \\ 0 \\ \vdots \end{bmatrix} = \frac{1}{d}\int_{-d/2}^{d/2} h(b(z,t)) \begin{bmatrix} \alpha_0(z) \\ \alpha_1(z) \\ \vdots \end{bmatrix} dz + \ldots$$

$$\ldots + \sigma d^2 \boldsymbol{C}\frac{\partial}{\partial t}\begin{bmatrix} b_0(t) \\ b_1(t) \\ \vdots \end{bmatrix}, \tag{8}$$

in which $\boldsymbol{C}$ is a constant matrix.

The constitutive material law combines a static hysteresis model and the excess-loss model of (2) applied locally in the lamination thickness:

$$h(b(z,t)) = h_\mathrm{hy}(b(z,t)) + \ldots$$

$$\ldots + c_{\text{ex}} \left| \frac{\partial b(z,t)}{\partial t} \right|^{-0.5} \frac{\partial b(z,t)}{\partial t}. \tag{9}$$

The static hysteretic part is modeled with a J-A hysteresis model [16]. In brief, the J-A model is described by the following five (differential) equations:

$$m = cm_{\text{an}} + (1-c)m_{\text{irr}} \tag{10a}$$

$$h_{\text{eff}} = h_{\text{hy}} + \alpha m \tag{10b}$$

$$m_{\text{an}} = m_{\text{s}} \left[\coth \frac{h_{\text{eff}}}{a} - \frac{a}{h_{\text{eff}}} \right] \tag{10c}$$

$$\frac{dm_{\text{irr}}}{dh_{\text{eff}}} = \frac{m_{\text{an}} - m_{\text{irr}}}{k\delta},\ \delta = \text{sign}\left(\frac{db}{dt}\right) \tag{10d}$$

$$\frac{dh_{\text{hy}}}{db} = \nu_0 \left(1 + \frac{dm}{dh_{\text{hy}}}\right)^{-1}, \tag{10e}$$

in which m, m_{an} and m_{irr} are the total, anhysteretic and irreversible magnetizations, respectively, h_{eff} is an effective field experienced by the domains, ν_0 is the vacuum reluctivity, and a, c, k, m_{s} and α are the constant parameters which should be identified from measurements.

The behavior of an unidirectional magnetic field in a ferromagnetic lamination is completely described by (8)-(10e). In this work, the equations were solved with a backward-Euler time-stepping scheme and using the Newton-Raphson method for the nonlinear iteration. $N_{\text{b}} = 2$ terms were used in the cosine series expansion (4) for the skin-effect modeling.

C. Anhysteretic Magnetization

To our experience, one of the main disadvantages of the J-A hysteresis model is its occasional inaccuracy in modeling the shapes of the hysteresis loops. This is mainly caused by the assumption of the hyperbolic cotangent shape of the $m_{\text{an}}(h_{\text{eff}})$ relationship in (10c). Since the material parameters are to be obtained by solving an inverse problem by comparison to measurements, we should be sure that the used hysteresis model is actually able to describe the material correctly. Thus we avoid using analytical expressions for the anhysteretic magnetization and instead replace the $m_{\text{an}}(h_{\text{eff}})$ relationship by the $\hat{m}(\hat{h}) = \nu_0 \hat{b}(\hat{h}) - \hat{h}$ curve extracted from the 50-Hz data used for the identification. This assumption is at least as reasonable as the assumption of the coth-shape, and allows reducing the total model parameters to five, since a and m_{s} are not needed.

D. Inverse-Problem Approach

After the anhysteretic magnetization curve is known, the five parameters of the model are $\boldsymbol{x} = (\sigma, c_{\text{ex}}, c, k, \alpha)$. The identification of the parameters can be formulated as an inverse problem in which the difference between the measured and simulated 50-Hz $\hat{h}(\hat{b})$ and $p(\hat{b})$ curves is minimized:

$$\tilde{\boldsymbol{x}} = \underset{\boldsymbol{x}}{\text{argmin}}\ F(\boldsymbol{x}) \tag{11a}$$

$$F(\boldsymbol{x}) = \left\| \frac{\hat{h}_{\text{meas}}(\hat{b}) - \hat{h}_{\text{sim}}(\boldsymbol{x}, \hat{b})}{\hat{h}_{\text{meas}}(\hat{b})} \right\|^2 + \ldots + \left\| \frac{p_{\text{meas}}(\hat{b}) - p_{\text{sim}}(\boldsymbol{x}, \hat{b})}{p_{\text{meas}}(\hat{b})} \right\|^2. \tag{11b}$$

This problem can be solved iteratively using global optimization algorithms.

Since the full numerical model (8)-(10e) is too slow to be used directly in the iterative procedure, a simple Kriging surrogate model was first built for fast emulation of the numerical model. The surrogate model was build based on 200 iron-loss simulations with different parameter values chosen using the Latin hypercube sampling method. After the optimal parameter values were solved from the inverse problem with the surrogate model, the full numerical model was ran with the obtained parameter values to verify the results.

III. Results

A. Unknown Conductivity

As the first attempt, the conductivity σ of the material was assumed to be unknown and was identified together with the other four parameters. The results are shown in Fig. 2. The simulated 50-Hz $\hat{h}(\hat{b})$ and $p(\hat{b})$ curves are very close to the measured ones. The rms errors between the measurements and simulations are 22 A/m and 0.158 W/kg, respectively. Also the 50-Hz hysteresis loops seem reasonable. However, the inverse problem solution gives a conductivity of $\sigma = 12.5$ MS/m, which is a clearly too large value for Fe-Si sheets. The effect of the exaggerated conductivity value is seen as severe overestimation of the losses at the higher frequencies.

B. Known Conductivity

Since fitting the conductivity lead to an unphysical value and incorrect estimation of the losses at higher frequencies, the next parameter identification was performed by fixing the conductivity to the measured value $\sigma = 2.96$ MS/m, while solving the remaining four parameters $\boldsymbol{x} = (c_{\text{ex}}, c, k, \alpha)$ from the inverse problem. The results are shown in Fig. 3. Again, the simulated 50-Hz single-valued magnetization and loss curves seem the be in good agreement with the measurements. The rms errors, 45.8 A/m and 0.194 W/kg, are somewhat larger than in the previous case. However, the 50-Hz hysteresis loops match even better with the measured ones. In addition, the high-frequency losses are estimated very accurately when compared to the measurements.

IV. Discussion and Conclusion

The parameters of a numerical iron-loss model were identified based on 50-Hz single-valued magnetization and loss-density curves which are typically available from electrical steel manufacturers. The identification was formulated as an inverse problem aiming to minimize the difference between measurements and numerical

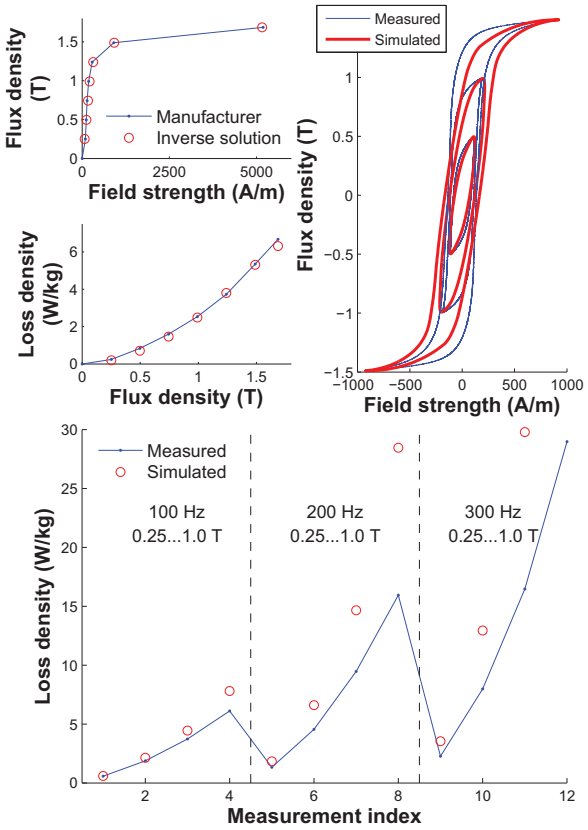

Fig. 2. Solution of the inverse problem with $\boldsymbol{x} = (\sigma, c_{\text{ex}}, c, k, \alpha)$, reconstructed 50-Hz hysteresis loops and high-frequency losses. The solved conductivity and excess-loss coefficient are $\sigma = 12.5$ MS/m, $c_{\text{ex}} = 0.403$ W/m^3(s/T)$^{1.5}$.

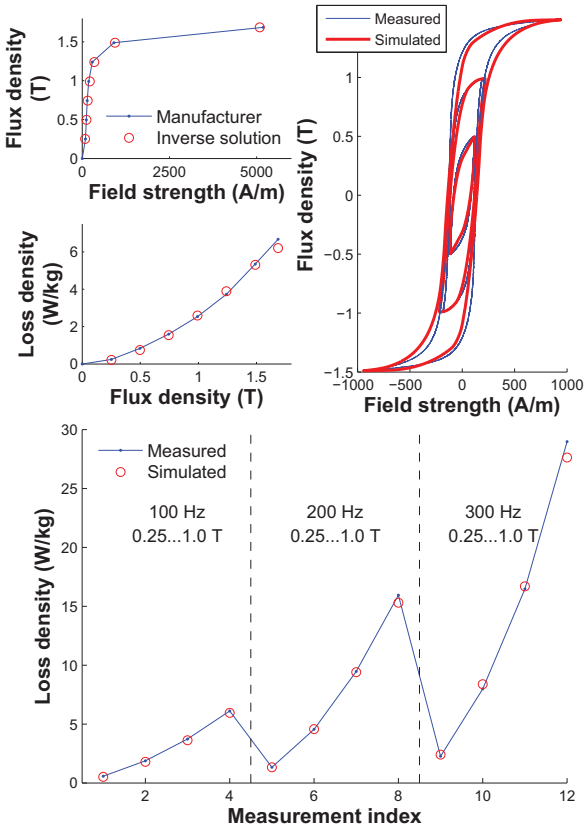

Fig. 3. Solution of the inverse problem with $\boldsymbol{x} = (c_{\text{ex}}, c, k, \alpha)$, reconstructed 50-Hz hysteresis loops and high-frequency losses. The conductivity is set to $\sigma = 2.96$ MS/m, the solved excess-loss coefficient is $c_{\text{ex}} = 0.872$ W/m^3(s/T)$^{1.5}$.

simulations. From the two studied cases, a better fit was obtained when the electrical conductivity was left unconstrained. However, this lead to an unphysically large value for the conductivity and a clear overestimation of the iron losses at higher frequencies. On the other hand, a very good loss-prediction accuracy was given by the parameter values obtained when the conductivity was forced to the measured value. In this case, however, the objective function was not in the minimum value.

Based on the results it is clear that the physically most reasonable solution is not necessarily the optimum from the objective-function point-of-view. In addition, the classical eddy-current and excess losses cannot be properly distinguished from each other at 50 Hz. Indeed, based on the results of Figs. 2 and 3, the excess-loss coefficient increases when the conductivity decreases. This implies a non-uniqueness in the inverse-problem solution if no a priori knowledge is available on the conductivity.

In the future, a more systematic study should be performed on the non-uniqueness and uncertainty related to the inverse-problem solution. Since this paper only focused on unidirectional excitation, the parameter identification results should also later be validated in the case of rotating magnetic fields.

REFERENCES

[1] C. P. Steinmetz, "On the law of hysteresis," Am. Inst. Electr. Eng. Trans. Vol. IX, No. 1, pp. 3-64, January 1892.

[2] G. Bertotti, "General properties of power losses in soft ferromagnetic materials," IEEE Trans. Magn., Vol. 24, No. 1, pp. 621-630, January 1988.

[3] J. Lammeraner, M. Štafl, "Eddy Currents," Iliffe Books, Prague, 1964.

[4] M. Albach, T. Durbaum A. Brockmeyer, "Calculating Core Losses in Transformers for Arbitrary Magnetizing Currents A Comparison of Different Approaches," in Proc. PESC, Vol. 2, pp. 1463-1468, Baveno, Italy, June 1996.

[5] I. Villar, A. Rufer, U. Viscarret, F. Zurkinden, I. Etxeberria-Otadui, "Analysis of Empirical Core Loss Evaluation Methods for Non-Sinusoidally Fed Medium Frequency Power Transformers," in Proc ISIE, Cambridge, UK, June-July 2008, pp. 208-213.

[6] J. Chen, W. MA, D. Wang, F. Li, Y. Guo, "A new method for calculating iron loss based on Hilbert transform," in Proc ICEM, Rome, Italy, September 2010, pp. 1-5.

[7] L.A. Righi, N. Sadowski, R. Carlson, J.P.A. Bastos, N.J. Batistela, "A new approach for iron losses calculation in voltage fed time stepping finite elements,", IEEE Trans. Magn., Vol. 37, No. 5, pp. 3353-3356, September 2001.

[8] P. Rasilo, E. Dlala, K. Fonteyn, J. Pippuri, A. Belahcen, and A. Arkkio, "Model of Laminated Ferromagnetic Cores for Loss Prediction in Electrical Machines," IET Electr. Power Appl., Vol. 5, No. 7, pp. 580-588, August 2010.

[9] E. Dlala, O. Bottauscio, M. Chiampi, M. Zucca, A. Belahcen, A. Arkkio, "Numerical Investigation of the Effects of Loading and Slot Harmonics on the Core Losses of Induction Machines," IEEE Trans. Magn., Vol. 48, No. 2, pp. 1063-1066, February 2012.

[10] I. Niyonzima, R. V. Sabariego, P. Dular, F. Henrotte, C. Geuzaine, "Computational Homogenization for Laminated Ferromagnetic Cores in Magnetodynamics," IEEE Trans. Magn., Vol. 49, No. 5, pp. 2049-2052, May 2013.
[11] P. Handgruber, A. Stermecki, O. Biró, A. Belahcen, E. Dlala, "Three-Dimensional Eddy-Current Analysis in Steel Laminations of Electrical Machines as a Contribution for Improved Iron-Loss Modeling," IEEE Trans. Ind. Appl., Vol. 49, No. 5, pp. 2044-2052, September/October 2013.
[12] F. Henrotte, S. Steentjes, K. Hameyer, C. Geuzaine "Iron Loss Calculation in Steel Laminations at High Frequencies," IEEE Trans. Magn., Vol. 50, No. 2, Art. no. 7008104, February 2014.
[13] E. Dlala "Efficient Algorithms for the Inclusion of the Preisach Hysteresis Model in Nonlinear Finite-Element Methods," IEEE Trans. Magn., Vol. 42, No. 2, pp. 395-408, February 2011.
[14] A. Abdallh, L. Dupré, "Magnetic material characterization using an inverse problem approach," book chapter in Advanced Magnetic Materials, ISBN 978-953-51-0637-1, InTech, 2012.
[15] P. Rasilo, A. Abdallh, A. Belahcen, A. Arkkio, L. Dupré, "Identification of Synchronous Machine Magnetization Characteristic from Calorimetric Core-Loss and No-Load Curve Measurements," IEEE Trans. Magn. (in press), August 2014.
[16] J. Gyselinck, P. Dular, N. Sadowski, J. Leite, and J. P. A. Bastos, "Incorporation of a Jiles-Atherton vector hysteresis model in 2D FE magnetic field computations," COMPEL, Vol. 23, No. 3, pp. 685-693, 2004.